Desalination and Water Treatment
www.deswater.com

doi: 10.5004/dwt.2019.23590

146 (2019) 227–235
April

Poly(lactic acid)/activated carbon composite beads by phase inversion method for kinetic and adsorption studies of Pb^{2+} ions in aqueous solution

Memoon Sattar[a], Fareeda Hayeeye[a], Watchanida Chinpa[b], Orawan Sirichote[a,*]

[a]*Department of Chemistry, Faculty of Science, Prince of Songkla University, Songkhla 90112, Thailand, Tel. (+66) 0896577950; email: orawan.si@psu.ac.th (O. Sirichote)*
[b]*Department of Materials Science and Technology, Faculty of Science, Prince of Songkla University, Songkhla 90112, Thailand*

Received 23 May 2018; Accepted 12 December 2018

ABSTRACT

Poly(lactic acid) (PLA)/activated carbon (AC) composite beads (PLA/AC beads) were prepared by a phase inversion technique to adsorb Pb^{2+} ions from an aqueous solution. In this work, the influence of various factors on the adsorption of pollutant Pb^{2+} ions were examined by batch equilibration. The effects of contact time, pH, adsorbent dosage, and initial concentration of Pb^{2+} ions were evaluated. The porous structure of the prepared PLA/AC beads was confirmed by scanning electron microscopy and nitrogen adsorption–desorption methods. The adsorption behavior of the developed PLA/AC beads followed the Langmuir and Freundlich adsorption isotherm models. However, the Langmuir model fitted better than the Freundlich model. The maximum adsorption capacity of the beads was 202.81 mg g^{-1} at pH 5 and 23°C±2°C. These results indicated that these PLA/AC beads could provide an alternative high-performance granular adsorbent for the removal of Pb^{2+} ions from polluted water.

Keywords: Adsorption isotherm; Activated carbon; Poly(lactic acid); Kinetics

1. Introduction

The environment continues to suffer from contamination with heavy metal ions. Since large amounts of Pb^{2+} and its compounds enter and permeate ecosystems in wastewater, they present a serious ongoing problem to the environment, human and animal health [1]. Thus, the extraction of Pb^{2+} ions from industrial wastewater is vital for the protection of environment, human, and animal health.

Several widely used methods for removing pollutants from industrial wastewater are in use: ion exchange [2,3], ultrafiltration [4], membrane processes [5] and adsorption [6–10]. Adsorption processes can remove pollutants such as cationic dyes [11], metals [12] and heavy metals [13–15], and activated carbon (AC) is an effective adsorbent used in these processes. In previous works, researchers studied the adsorption of Pb^{2+} ions by AC powder prepared from apricot stones [16], palm shells [17] and walnut wood [18]. However, AC in fine powder form has a limited capacity. Adsorption of Pb^{2+} ions on recently developed granular AC was more effective than adsorption on powdered AC. Granular AC has been made from materials such as coconut shell [19], cherry stones [20] and hydroxyapatite granular AC nanocomposite [21]. However, these granular adsorbents could not be prepared in a simple way and require toxic reagents. In this study, AC was compacted into bead form with poly(lactic acid) (PLA) to create an efficient granular adsorbent that is easier to use than AC in powder form. PLA was chosen for this work because it is biodegradable, environmentally friendly, thermoplastic aliphatic polyester from renewable resources. Its structure is shown in Fig. 1. In this work, PLA/AC beads were prepared by a simple phase inversion technique. The concept of phase inversion covers a range of different techniques such as precipitation by controlled evaporation, thermal precipitation from the vapor phase and immersion precipitation [22]. This technique has been

* Corresponding author.

1944-3994/1944-3986 © 2019 Desalination Publications. All rights reserved.

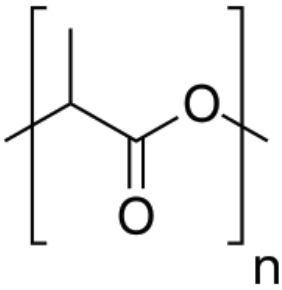

Fig. 1. Chemical structure of PLA.

extensively described in the literature for a large number of polymer/solvent/nonsolvent combinations [23–25]. In the present work, the immersion precipitation method or wet process was used to prepare PLA/AC beads using N-methyl-2-pyrrolidone (NMP) and water as solvent and nonsolvent, respectively. The aim of this research is to optimize various factors such as contact time, pH and PLA/AC dose and to evaluate the kinetic adsorption isotherms of Pb^{2+} ions onto PLA/AC composite beads. The aims were achieved and the expected advantages, convenience and high adsorption capacity of PLA/AC composite in bead form indicate that it may be an eco-friendly, alternative adsorbent for water treatment.

2. Materials and methods

2.1. Materials and reagents

Poly(lactic acid) (PLA) and AC were purchased from NatureWorks (USA) and Sigma-Aldrich (UK), respectively. NMP, used as a solvent, was purchased from RCI Labscan limited (Thailand). The PLA/AC beads were prepared by the following phase inversion method: a 10% w/v PLA solution was prepared in NMP. Then, 5% w/v AC was added into the PLA solution and stirred at room temperature for 24 h. The PLA/AC solution was added drop wise into the nonsolvent (distilled water) and the beads formed immediately. Later, the PLA/AC beads were washed six or seven times with double distilled water and finally dried in an oven at 60°C for 6 h [26]. Lead salt ($PbNO_3$), procured to prepare an aqueous solution of the adsorbent ion (Pb^{2+}), was purchased from UNILAB (United Kingdom). When necessary, the pH of the standard solutions was adjusted with NaOH or HCl (Merck, Germany).

2.2. Characterization of the PLA/AC beads

Characterization of the PLA/AC beads was carried out using an Autosorb-1-MP analyzer (Quantachrome Instruments, FL, USA) at the Science and Technology Service Center of Chiang Mai University (STSC-CMU). The Brunauer–Emmett–Teller (BET) equation [27] and the Barrett–Joyner–Halenda (BJH) model [28] were applied to determine the surface area and the pore size distribution of the PLA/AC beads, respectively.

In physical chemistry, the point of zero charge (pH_{pzc}) is a concept relating to the phenomenon of adsorption. It describes the condition at which the electrical charge density on a surface is zero [29]. Here, pH_{pzc} was determined using the pH drift method [30] as follows: the pH of 0.1 M NaCl solution 50 mL was adjusted to a value between 2 and 12 using 0.1 M HCl or 0.1 M NaOH; PLA/AC (0.25 g) was added into each of the pH-adjusted solutions and equilibrated for 24 h; final pH was measured and plotted against initial pH and the pH at which the curve crossed the line $pH_f = pH_0$ was taken as the pH_{pzc} of the PLA/AC beads [31].

Scanning electron microscopy (SEM) and energy dispersive X-ray spectroscopy (EDX) were used to study the external morphology of the PLA/AC beads. Images were obtained using a Quanta 400 scanning electron microscope at the Scientific Equipment Center (Prince of Songkla University).

2.3. Batch equilibration method

The adsorption of Pb^{2+} ions by the developed PLA/AC beads was carried out by the batch equilibration method [32]. All experiments and mean values including standard deviations were reported in triplicates. The variable parameters selected were contact time (0–180 min), pH (1.5–5.5), and amount of PLA/AC beads (0.1–0.5 g). The effects of varying these parameters were observed. To determine the effect of pH, the initial pH of the Pb^{2+} ions was adjusted to the desired value between 1.5 and 5.5 with HCl or NaOH solution. In the adsorption study, 0.25 g of PLA/AC was added into 50 mL samples of Pb^{2+} ions at 100–4,000 mg L^{-1} of solution at pH 5.0. The mixture was agitated in a rotary shaker at 23°C±2°C for 180 min. The concentration of Pb^{2+} ions, before and after adsorption, was determined by atomic absorption spectrophotometry. For the selective adsorption test, mixed solutions of Pb^{2+}, Cu^{2+}, Cd^{2+}, Zn^{2+} and Mn^{2+} ions at pH 5.0 were prepared, and initial concentrations of all metal ions were 50 and 100 mg L^{-1}.

2.4. Mathematical treatment for kinetic and adsorption studies

2.4.1. Determination of adsorbed amount of Pb^{2+} ions

Pb^{2+} ion concentration was analyzed by atomic absorption spectrophotometry. The adsorbed amount of Pb^{2+} ions was calculated from Eq. (1) and the percentage of Pb^{2+} ions adsorbed was determined with Eq. (2) as follows [33]:

$$q_e = \frac{V(C_0 - C_e)}{W} \tag{1}$$

and

$$\%Pb^{2+}\ \text{adsorbed} = \frac{C_0 - C_e}{C_e} \times 100 \tag{2}$$

where q_e is the amount of Pb^{2+} ions adsorbed (mg g^{-1}) in solid phase at equilibrium, V is the volume of the solution (L), C_0 is the initial concentration of Pb^{2+} ions (mg L^{-1}), C_e is the equilibrium concentration of Pb^{2+} ions (mg L^{-1}), and W is the mass of adsorbent (g).

Kinetic adsorption and adsorption isotherms were evaluated from the equilibrium data. The maximum adsorption

capacities were calculated using the Langmuir model for monolayer saturation of Pb^{2+} ions on PLA/AC beads.

2.4.2. Kinetic models

The kinetic models of Pb^{2+} ions sorption used were pseudo-first order [34,35] and pseudo-second order [36] kinetic models, as shown in Eqs. (3) and (4), respectively.

$$\frac{dq_t}{dt} = k_1(q_e - q_t) \tag{3}$$

$$\frac{dq_t}{dt} = k_2(q_e - q_t)^2 \tag{4}$$

where q_t is the amount of Pb^{2+} ions adsorbed (mg g^{-1}) at a given time t, k_1, and k_2 are, respectively, the pseudo-first order and pseudo-second order kinetic constants, and q_e is the amount of Pb^{2+} ions adsorbed (mg g^{-1}) in solid phase at equilibrium (mg g^{-1}).

2.4.3. Adsorption isotherm models

The Langmuir adsorption isotherm [37,38] is often used to describe adsorption on homogeneous surfaces based on the assumptions of monolayer adsorption. The Freundlich adsorption isotherm [39] is used for non-ideal adsorption, which involves systems with heterogeneous surface energy. It is assumed that adsorption occurs at sites of different energy. The isotherms were derived from Eqs. (5) and (6), respectively:

$$q_e = \frac{q_m b C_e}{1 + bC_e} \tag{5}$$

$$q_e = K_F C_e^{1/n} \tag{6}$$

where C_e is the equilibrium concentration of adsorbate in solution (mg L^{-1}), q_e is the equilibrium concentration of adsorbate in the adsorbent (mg g^{-1}), and q_m and b are Langmuir constants related to the maximum adsorption capacity (mg g^{-1}) and the adsorption equilibrium constant (L mg^{-1}), respectively; K_F and n are Freundlich constants related to the adsorption capacity and the adsorption intensity, respectively.

2.4.4. Dimensionless separation factor (R_L)

For the Langmuir isotherm model, the dimensionless separation factor (R_L) [40,41] can be used to predict the favorability of adsorption, which is calculated from Eq. (7):

$$R_L = \frac{1}{1 + bC_0} \tag{7}$$

R_L values indicate the nature of adsorption to be unfavorable ($R_L > 1$), linear ($R_L = 1$), favorable ($0 < R_L < 1$), or irreversible ($R_L = 0$).

2.4.5. Selectivity coefficient

The selectivity of PLA/AC beads for Cu^{2+} over the other metal ions can be estimated by the selectivity coefficient (Cu^{2+}/M^{2+}), which is expressed as Eq. (8):

$$\beta_{Cu^{2+}/M^{2+}} = \frac{D_{Cu^{2+}}}{D_{M^{2+}}}; \qquad D = \frac{C_0 - C_e}{C_e} \times \frac{V}{W} \tag{8}$$

$D_{Cu^{2+}}$ and $D_{M^{2+}}$ are the distribution ratio (D) of the Cu^{2+} and other coexisting metal ions, respectively, C_0 and C_e are the initial concentration of metal ions (mg L^{-1}), V is the volume of the solution (L), and W is the mass of PLA/AC beads (g).

3. Results and discussion

3.1. Characterization of PLA/AC bead

The specific surface area of the prepared PLA/AC beads, determined from the BET equation [27] was 95.98 $m^2 g^{-1}$. The pore size distribution of the beads, which was relatively narrow, was determined by the BJH model [28]. The PLA/AC beads presented an average pore diameter of 3.34 nm. This result indicates that the developed beads may be classified as a mesoporous material, containing pores with diameters between 2 and 50 nm [42]. Furthermore, the point of zero charge (pH_{pzc}) of the PLA/AC beads was 3.5 indicative of a surface of an acidic nature.

The digital photograph in Fig. 2(a) shows spherical PLA/AC beads of nearly equal size. SEM images of PLA/AC beads are shown in Figs. 2(b)–(d). The spherical PLA/AC bead in Fig. 2(b) shows a diameter of about 3 mm. The numerous pores on the surface of the PLA/AC bead (Fig. 2(c)) and the internal cross-section (Fig. 2(d)) are clearly presented.

3.2. Adsorption studies

3.2.1. Effect of contact time and initial Pb^{2+} ions concentration

The time to reach equilibrium is a necessary datum for the study of kinetic adsorption [43–46]. The amount of adsorbate adsorbed at time t, q_t, was used to determine the kinetic models. Graphs were plotted of q_t against t for all three initial concentrations of Pb^{2+} ions (50, 300, and 500 mg L^{-1}) at 23°C±2°C, pH 5.0 and 0.25 g dose of PLA/AC. The plots show that sorption of Pb^{2+} ions increased by increasing the concentration of Pb^{2+} ions in solution (Fig. 3). But the different initial concentrations did not affect the time to reach equilibrium. It was found that the uptake equilibrium of Pb^{2+} ions on PLA/AC beads was achieved after 60 min and no significant changes were observed for longer times (Fig. 3). As expected, the amount adsorbed increased with initial Pb^{2+} ions concentration. The shapes of the curves representing Pb^{2+} ions uptake vs. time suggest two adsorption steps. The first step, occurring during the first 30 min, indicated a rapid adsorption after which equilibrium was slowly achieved. In 50, 300, and 500 mg L^{-1} initial concentrations of Pb^{2+}, approximately 83.85%, 78.79% and 71.77%, respectively, of the total final removal of Pb^{2+} ions occurred within 60 min. Consequently, 180 min was chosen to ensure equilibrium in the kinetic studies and determination of the adsorption isotherms.

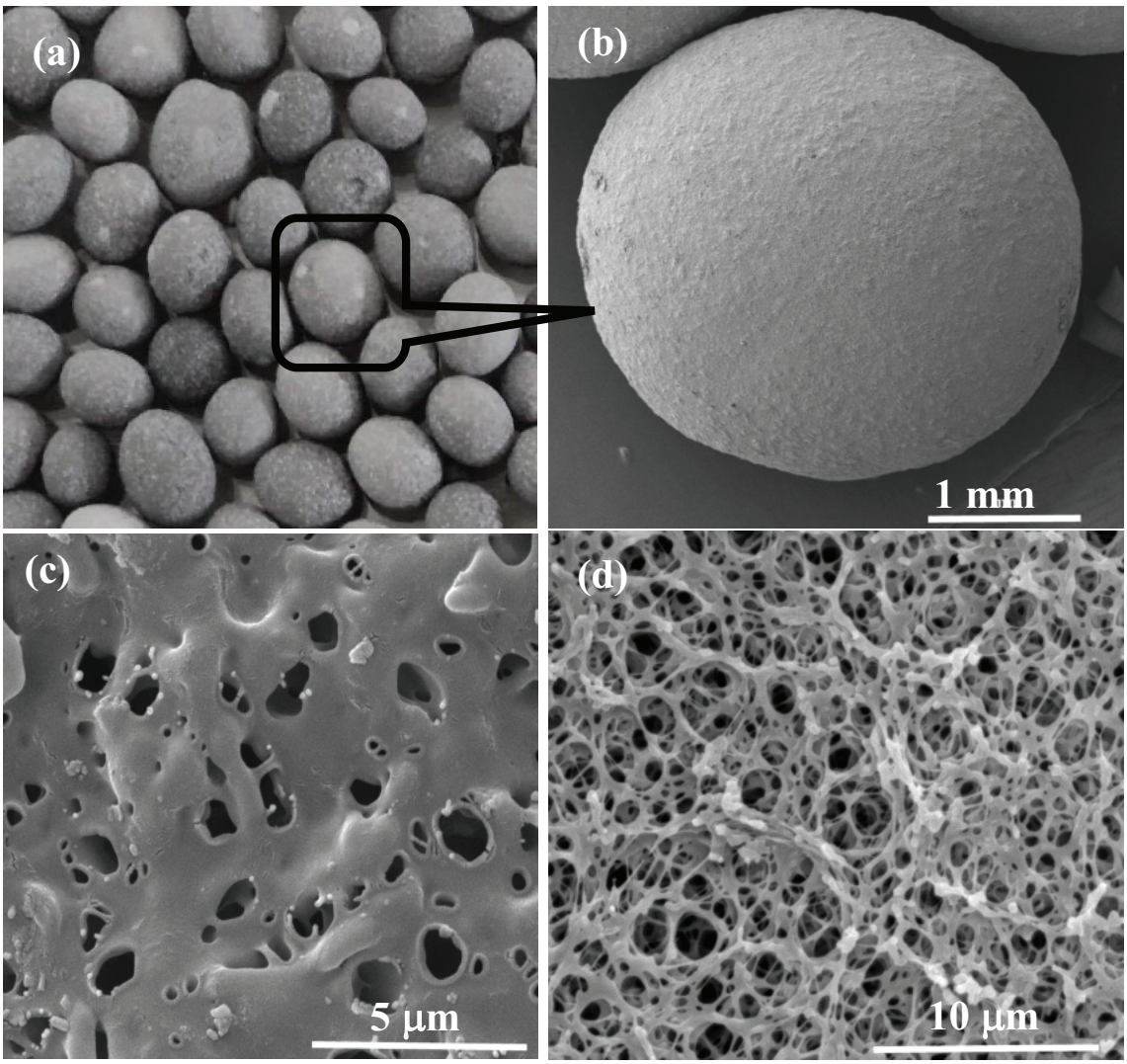

Fig. 2. (a) Digital photograph of PLA/AC beads and SEM images of (b) bead size, (c) surface, and (d) internal cross-section of PLA/AC bead.

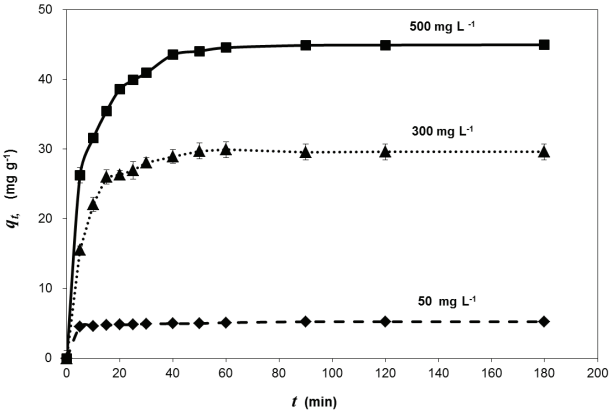

Fig. 3. Effect of contact time of Pb^{2+} ions adsorption onto PLA/AC beads at different initial Pb^{2+} ions concentrations (50, 300, and 500 mg L^{-1}). PLA/AC dose 0.25 g/50 mL, temperature 23°C±2°C, and pH = 5.

In order to analyze the adsorption kinetics of Pb^{2+} ions on PLA/AC beads, two kinetic models were applied to the experimental data. Figs. 4(a) and (b) show the plots of non-linear forms of pseudo-first order and pseudo-second order kinetic models at all initial concentrations. The kinetic models for adsorption of Pb^{2+} ions on PLA/AC beads were also tested to obtain the rate parameters according to Eqs. (3)–(6). Kinetic parameters (q_{exp}, k_1 and k_2) for two kinetic models and correlation coefficients of Pb^{2+} ions on PLA/AC beads under different initial concentrations of Pb^{2+} ions were calculated and are displayed in Table 1.

The validity of these kinetic models was checked. The plots in Figs. 4(a) and (b) show a good agreement of dynamical data, corresponding to the pseudo-second order kinetic model. The correlation coefficient values (R^2) of the pseudo-second order kinetic model for Pb^{2+} ions on PLA/AC beads are extremely high ($R^2 > 0.99$) (Table 1). Moreover, the equilibrium sorption capacities derived from the pseudo-second order model were much closer to the experimental results than those of the pseudo-first order system.

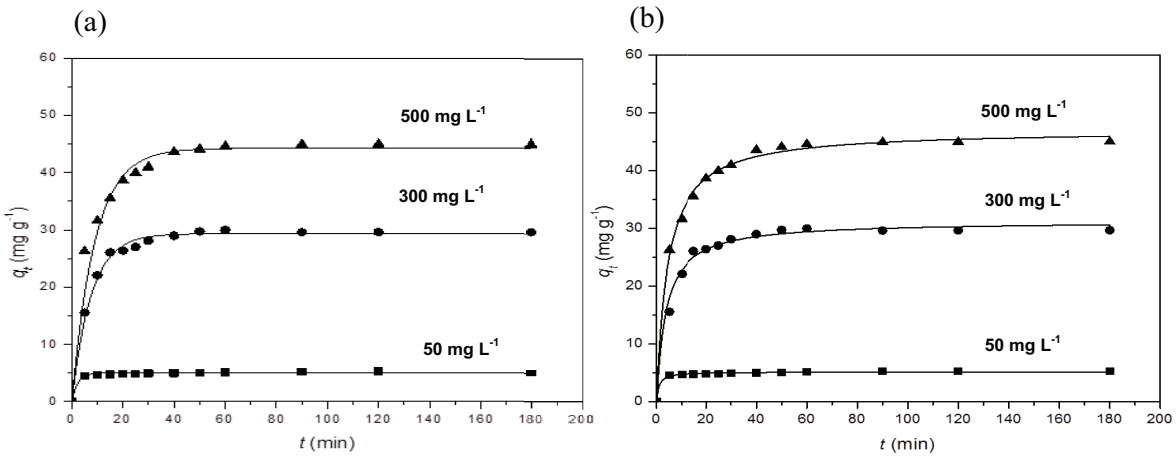

Fig. 4. (a) Pseudo-first order and (b) pseudo-second order kinetic models for Pb^{2+} ions adsorption onto PLA/AC beads. PLA/AC dose 0.25 g/50 mL, temperature = 23°C±2°C, pH = 5 and equilibrium time = 180 min.

Table 1
Parameters of kinetic studies of the pseudo-first order and the pseudo-second order models with various initial concentrations of Pb^{2+} ions (50, 300 and 500 mg L^{-1}) at 23°C±2°C, PLA/AC dose 0.25 g, and pH = 5, equilibrium time 180 min.

C_0 (mg L^{-1})	q_e (exp) (mg g^{-1})	Pseudo-first order			Pseudo-second order		
		q_e (mg g^{-1})	k_1 (×10^{-1}) (min^{-1})	R^2	q_e (mg g^{-1})	k_2 (×10^{-3}) (g mg^{-1} min^{-1})	R^2
50	5.25	4.89	4.38	0.991	5.15	2.13	0.995
300	29.57	29.11	1.32	0.987	31.20	8.61	0.999
500	44.90	43.27	1.11	0.981	45.01	4.89	0.998

3.2.2. Effect of pH

In Fig. 5, the pH of the system is an important variable parameter in the adsorption process because the surface charge of the adsorbent often depends on the pH of the solution. The adsorption capacity of the developed PLA/AC beads for Pb^{2+} ions increased across the pH range as the pH was increased from 1.5 to 5.5. The lower adsorption capacity observed at lower solution pH might occur because, at low pH values, the high concentration of H^+ ions promotes the protonation of functional groups, such as carboxylic groups, in the adsorbent. As a result, these functional groups become positively charged and repel the positive charges of the cationic Pb^{2+} ions: hence result in the reduction of Pb^{2+} ions adsorption. An alternative view is that, at such low pH values, the H^+ ions compete with Pb^{2+} ions for adsorption sites [16].

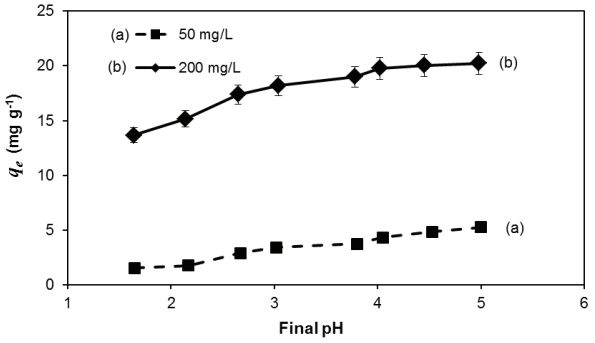

Fig. 5. Effect of pH on PLA/AC beads for Pb^{2+} ions adsorption. PLA/AC dose 0.25 g/50 mL, temperature 23°C±2°C, Pb^{2+} concentration of (a) 50 mg L^{-1} and (b) 200 mg L^{-1}.

3.2.3. Adsorption isotherms

The isotherm parameters from nonlinear regression of the equilibrium data of Pb^{2+} ions sorption on PLA/AC beads indicate the L-2 type isotherm (Fig. 6). This type represents the ratio between the concentrations of Pb^{2+} ions remaining in solution and adsorbed on the PLA/AC beads decreasing as increase in Pb^{2+} ions concentration. This produces a concave curve [47]. This indicated that there was a reduction in the number of active sites on the adsorbent surface at higher Pb^{2+} ions concentration in the solution phase.

Fig. 7 shows the adsorption isotherms of Langmuir and Freundlich models for Pb^{2+} ions adsorption onto PLA/AC beads at 23°C±2°C, from initial concentrations of 100 to 4,000 mg L^{-1} and pH range 3 to 5. Moreover, all of the fitted parameters are summarized in Table 2.

The favorability of adsorption is known to be indicated by the dimensionless separation factor (R_L). Calculated from the data in Table 2, the R_L values were 0.07–0.80 at pH 3, 4, and 5 in the initial concentration range of 100–4,000 mg L^{-1}. These values suggested that the Langmuir isotherm is favorable. The obtained results revealed that the equilibrium data of Pb^{2+} ions sorption on PLA/AC beads were well described by both Langmuir and Freundlich models but, of the two models, the Langmuir model performed better, producing higher R^2 values (Table 2), indicating a monolayer adsorption mechanism.

The maximum Pb^{2+} ions uptake capacities (q_m, mg g^{-1}) of the developed PLA/AC beads were compared with those of other adsorbents reported in the literature (Table 3). The maximum adsorption capacity of PLA/AC beads for Pb^{2+} ions was higher than all of the adsorbents in the literature.

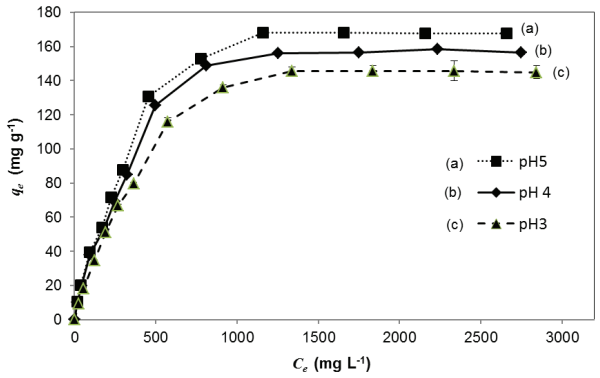

Fig. 6. Adsorption isotherms of Pb^{2+} ions onto PLA/AC beads. PLA/AC dose = 0.25 g/50 mL, temperature = 23°C±2°C; pH = 3, 4, and 5; and equilibrium time = 180 min.

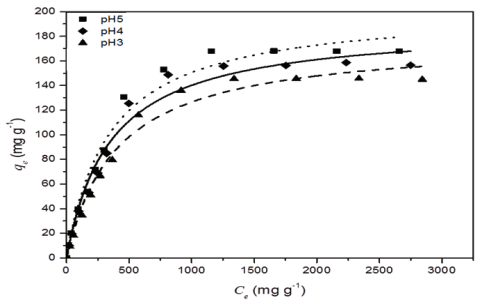

Fig. 7. Adsorption isotherms of Langmuir model for Pb^{2+} ions adsorption onto PLA/AC beads. pH = 3, 4, and 5; temperature = 23°C±2°C; PLA/AC dose = 0.25 g; and equilibrium time = 180 min.

3.2.4. Effect of PLA/AC dosage

The adsorption of Pb^{2+} ions increased as a function of the dosage of PLA/AC beads. For initial concentrations of Pb^{2+} ions of 100, 200, and 300 mg L^{-1}, the percent adsorption of Pb^{2+} ions increased, respectively, from 41% to 80%, from 44% to 84%, and from 55% to 85% from the initial adsorbent dosage of 0.1 g/50 mL to the final dosage of 0.4 g/50 mL (Fig. 8). This increased adsorption was due to the increasing number of binding sites for complexation of Pb^{2+} ions. Thus, the PLA/AC beads dosage is another important parameter which influences the extent of Pb^{2+} ions uptake from the solution. The percentage of Pb^{2+} ions adsorbed reached a maximum value when the weight of PLA/AC beads was 0.4 g. However, after 0.25 g, the adsorption capacity only slightly increased with increments of PLA/AC beads. A dosage of 0.25 g was, therefore, considered to be the optimum level for the PLA/AC beads. Also, at this dosage, the time to reach equilibrium was short, which is advantageous in industrial applications [55].

Table 2
Parameters of the Langmuir and Freundlich models for Pb^{2+} ions adsorption by PLA/AC beads (0.25 g) at 23°C±2°C, pH = 3, 4 and 5 and equilibrium time = 180 min

pH	Langmuir			Freundlich		
	q_m (mg g^{-1})	b (L mg^{-1})	R^2	K_F (mg g^{-1})	n	R^2
3	177.55	0.0024	0.999	2.00	1.71	0.929
4	189.25	0.0028	0.998	2.91	1.78	0.938
5	202.81	0.0029	0.999	2.71	1.79	0.932

Table 3
Maximum adsorption capacities of Pb^{2+} ions compared with other adsorbents reported in the literature

S. No.	Adsorbent	pH	q_m (mg g^{-1})	Ref.
1	Apricot stone activated carbon	5.0	22.84	[16]
2	Palm shell activated carbon with chelating polymer	5.0	20.00	[17]
3	Walnut wood activated carbon	5.0	47.62	[18]
4	Nano hydroxyapatite (HAp) and hydroxyapatite granular activated carbon nanocomposite (C-HAp)	6.0	HAp = 83.83 C-HAp = 9.31	[21]
5	Pure chitosan (PC) and goethite/chitosan nanocomposite (GC)	6.0	PC = 36.61 GC = 61.51	[48]
6	Chitin nanofibers (CNFs) and chitosan nanoparticles (CNPs)	5.0	CNFs = 60.24 CNPs = 94.34	[49]
8	Magnetic ATP/FA/Poly(AA-co-AM) ternary nanocomposite microgel	5.0	40.0	[50]
9	Magnetic Fe_3O_4@ silica–xanthan gum composites	6.0	20.32	[51]
10	Magnetic chitosan (MC), graphene oxide (GO), and magnetic chitosan/graphene oxide imprinted Pb^{2+} (Pb-MCGO)	6.0	MC = 47.91 GO = 45.23 Pb-MCGO = 79.80	[52]
11	Lanthanide metal–organic frameworks	6.5	5.07	[53]
12	Natural adsorbent perlite	6.0	31.25	[54]
13	Polylactic acid/activated carbon composite bead form (PLA/AC)	5.0	202.81	This study

3.2.5. Selective adsorption test

For the selective adsorption test, a mixed solution containing Pb^{2+}, Cu^{2+}, Cd^{2+}, and Zn^{2+} ions was prepared. The concentration of all heavy metal ions to be adsorbed by the PLA/AC beads was set at 50 mg L^{-1}. The adsorption of Cu^{2+} ion was higher than the other heavy metals in the mixed solution and the order of adsorbed percentages is $Cu^{2+} > Pb^{2+} > Cd^{2+} > Zn^{2+} > Mn^{2+}$ (Fig. 9). Preferential adsorption of heavy metal ions depends on many factors, such as initial concentration, adsorbent species and dosages. The selectivity of the PLA/AC beads for Cu^{2+} over the other metal ions was estimated from the selectivity coefficients calculated from Eq. (8) (Table 4). It can be seen from the results that the relative selectivity coefficients for each specific metal ion are far greater than 1, indicating priority of sorption of the corresponding ion and ability to remove other metal species in a mixed solution [56].

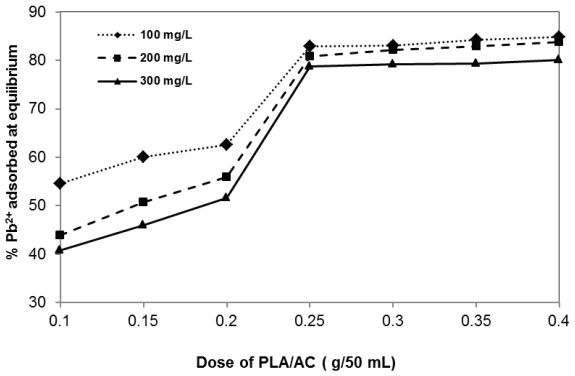

Fig. 8. Effect of dosage on PLA/AC beads for Pb^{2+} ions adsorption. PLA/AC dose = 0.1–0.4 g/50 mL, temperature = 23°C±2°C; pH = 5; and initial Pb^{2+} ions concentration of 100, 200, and 300 mg L^{-1}.

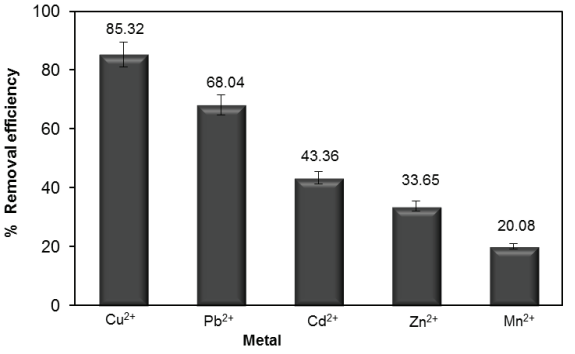

Fig. 9. Percentage efficiency of metal ions removal on PLA/AC beads from a mixed solution of metal ions (C_0 = 50 mg L^{-1}, pH = 5.0).

Table 4
Selective adsorption of Pb^{2+}, Cu^{2+}, Cd^{2+}, Zn^{2+}, and Mn^{2+} ions on PLA/AC beads

Metal ions	Distribution ratio (L g^{-1})	Selectivity coefficient
Cu^{2+}	1.162	–
Pb^{2+}	0.136	8.542
Cd^{2+}	0.087	13.404
Zn^{2+}	0.067	17.272
Mn^{2+}	0.040	28.944

Derived from an energy dispersive X-ray spectrometer system (SEM/EDX), using a standardless qualitative EDX analytical technique, the EDX spectra and dot mapping of a PLA/AC bead before and after adsorption of Pb^{2+} ions are presented in Fig. 10. The qualitative spectra of the PLA/AC bead before adsorption, shown in Fig. 10(a), indicated that C and O are the main components. The single of the Pb element in the PLA/AC bead was represented by the bright points in the dot mapping. After Pb^{2+} ions adsorption, the EDX spectrum of the PLA/AC bead showed main components of C, O, and Pb (Fig. 10(b)). The presence of Pb^{2+} ions in the spectrum confirmed the adsorption of Pb^{2+} ions on the PLA/AC bead. Moreover, the elemental distribution mapping of adsorbed Pb^{2+} ions on the PLA/AC bead clearly presented, by dot mapping, the distribution of Pb^{2+} ions on the surface of PLA/AC bead (Fig. 10(b)).

4. Conclusions

Efficient, cheap, and eco-friendly PLA/AC beads were successfully prepared by a facile method for use as a potential adsorbent for the removal of Pb^{2+} ions from aqueous solutions. The PLA/AC beads presented a highly porous spherical form in mesoporous scale. The kinetic adsorption of the developed composite beads was successfully described by the pseudo-second order kinetic model. Moreover, Langmuir

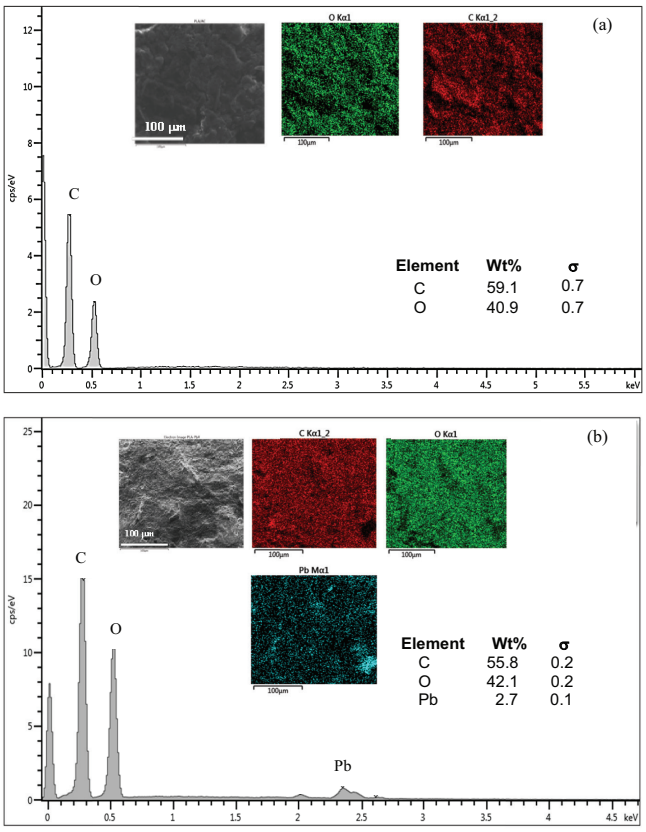

Fig. 10. EDX spectra and dot mapping of PLA/AC bead (a) before and (b) after Pb^{2+} ions adsorption.

and Freundlich isotherm models were evaluated and the equilibrium data were best fitted by the Langmuir model. The maximum adsorption capacity (q_{max}) was 202.81 mg g^{-1} at pH 5.0, temperature 23°C±2°C and PLA/AC dose 0.25 g. From these results, it can be concluded that the PLA/AC beads are not only more convenient to use than powder AC but also their higher adsorption capacity for the removal of Pb^{2+} ions will be useful in the process of industrial wastewater treatment.

Acknowledgments

This research was supported by the PSU Ph.D. Scholarship from the Graduate School, Prince of Songkla University and Department of Chemistry, Faculty of Science, Prince of Songkla University, Hat Yai campus. The authors would also like to greatly appreciate Faculty of Science Research Fund Year 2015, 158004. Moreover, they would like to acknowledge Dr. Laemthong Chuenchom and Mr. Natthanan Rattanachueskul for analyzing the data using OriginPro program. They are thankful to Mr. Thomas Duncan Coyne for assistance with English.

References

[1] S. Tiwari, I.P. Tripathi, H.L. Tiwari, Effects of lead on environment, Int. J. Emer. Res. Manage. Technol., 2 (2013) 1–5.
[2] J.R. Li, X. Wanga, Y. Baoling, F. Ming-Lai, Layered chalcogenide for Cu^{2+} removal by ion-exchange from wastewater, J. Mol. Liq., 200 (2014) 205–212.
[3] G. Bayramoğlu, G. Ekici, N. Beşirli, M.Y Arica, Preparation of ion-exchange beads based on poly(methacrylic acid) brush grafted chitosan beads: isolation of lysozyme from egg white in batch system, Colloids Surf., A, 310 (2007) 68–77.
[4] M. Hébrant, M. Rose-Hélène, A. Walcarius, Metal ion removal by ultrafiltration of colloidal suspensions of organically modified silica, Colloids Surf. A, 417 (2013) 65–72.
[5] L.M. Ortega, R. Lebrun, J.F. Blais, R. Hausler, Treatment of an acidic leachate containing metal ions by nanofiltration membranes, Sep. Purif. Technol., 54 (2007) 306–314.
[6] I.H. Liao, J.H. Huang, S.L. Wang, M.P. Cheng, J.C. Liu, Adsorptions of Cd(II) and Pb(II) in aqueous solution by rice-straw char, Desal. Wat. Treat., 57 (2016) 21619–21626.
[7] Chandran Prince Jebadass Isaac, A. Sivakumar, Removal of lead and cadmium ions from water using *Annona squamosa* shell: kinetic and equilibrium studies, Desal. Wat. Treat., 51 (2013) 7700–7709.
[8] M. Belhachemi, F. Addoun, Adsorption of congo red onto activated carbons having different surface properties: studies of kinetics and adsorption equilibrium, Desal. Wat. Treat., 37 (2012) 122–129.
[9] C. Wang, H. Wang, Y. Liu, Purification of Pb (II) ions from aqueous solution by camphor leaf modified with succinic anhydride, Colloids Surf. A, 509 (2016) 80–85.
[10] Y.H. Li, S. Wang, J. Wei, X. Zhang, C. Xu, Z. Luan, D. Wu, B. Wei, Lead adsorption on carbon nanotubes, Chem. Phys. Lett., 357 (2002) 263–266.
[11] A. Bhatnagar, A.K. Jain, A comparative adsorption study with different industrial wastes as adsorbents for the removal of cationic dyes from water, J. Colloid Interface Sci., 281 (2005) 49–55.
[12] K. Wilson, H. Yang, C.W. Seo, W.E. Marshall, Select metal adsorption by activated carbon made from peanut shells, Bioresour. Technol., 97 (2006) 2266–2270.
[13] L. Chuenchom, Adsorption of Cadmium (II) and Lead (II) Ions on Activated Carbons Obtained from Bagasse and Pericarp of Rubber Fruit, Master of Science Thesis in Physical Chemistry, Prince of Songkla University, 2004.
[14] G.E. Sharaf El-Deen, S.E.A. Sharaf El-Deen, Kinetic and isotherm studies for adsorption of Pb(II) from aqueous solution onto coconut shell activated carbon, Desal. Wat. Treat., 57 (2016) 28910–28931.
[15] X. Lu, J. Jiang, K. Sun, G. Zhu, G. Lin, Enhancement of Pb^{2+} removal by activating carbon spheres/activated carbon composite material with H_2O vapor, Colloids Surf. A, 506 (2016) 637–645.
[16] M. Kobya, E. Demirbas, E. Senturk, M. Ince, Adsorption of heavy metal ions from aqueous solutions by activated carbon prepared from apricot stone, Bioresour. Technol., 96 (2005) 1518–1521.
[17] M.K. Aroua, C.Y. Yin, F.N. Lima, W.L. Kana, W.M. Ashri, Effect of impregnation of activated carbon with chelating polymer on adsorption kinetics of Pb^{2+}, J. Hazard. Mater., 166 (2009) 1526–1529.
[18] M. Ghaedi, H. Mazaheri, S. Khodadoust, S. Hajati, M.K. Purkait, Application of central composite design for simultaneous removal of methylene blue and Pb^{2+} ions by walnut wood activated carbon, Spectrochim. Acta Part A, 135 (2015) 479–490.
[19] J. Goel, K. Kadirvelu, C. Rajagopal, V.K. Garg, Removal of lead (II) by adsorption using treated granular activated carbon: batch and column studies, J. Hazard. Mater., B125 (2005) 211–220.
[20] J. Jaramillo, V. Gómez-Serrano, P.M. Alvarez, Enhanced adsorption of metal ions onto functionalized granular activated carbons prepared from cherry stones, J. Hazard. Mater., 161 (2009) 670–676.
[21] M.S. Fernando, R.M. de Silva, K.M. Nalin de Silva, Synthesis, characterization, and application of nano hydroxyapatite and nanocomposite of hydroxyapatite with granular activated carbon for the removal of $Pb^{2+}$from aqueous solutions, Appl. Surf. Sci., 351 (2015) 95–103.
[22] M. Mulder, Membrane Preparation/Phase Inversion Membranes, University of Twente, Enschede, The Netherlands, 2000, pp. 3331–3345.
[23] A. Figoli, G.D. Luca, E. Longavita, E. Drioli, PEEKWC capsules prepared by phase inversion technique: a morphological and dimensional study, Sep. Sci. Technol., 42 (2007) 2809–2827.
[24] J.G. Wijmans, J. Kant, M.H. Mulder, C.A Smolders, Phase separation phenomena in solutions of polysulfone in a mixture of a solvent and a nonsolvent: relationship with membrane formation, Polymer, 26 (1985) 1539.
[25] C.A. Smolders, A.J. Reuvers, R.M. Boom, I.M. Wienk, Microstructures in phase inversion membranes, Part 1. Formation of macrovoids, J. Membr. Sci., 73 (1992) 259.
[26] M. Sattar, F. Hayeeye W. Chinpa, O. Sirichote, Preparation and characterization of poly (lactic acid)/activated carbon composite bead via phase inversion method and its use as adsorbent for Rhodamine B in aqueous solution, J. Environ. Chem. Eng., 5 (2017) 3780–3791.
[27] S. Brunauer, P. Emmett, E. Teller, Adsorption of gases in multimolecular layers, J. Am. Chem. Soc., 60 (1938) 309–319.
[28] E.P. Barrett, L.G. Joyner, P.P. Halenda, The determination of pore volume and area distributions in porous substances I. Computations from Nitrogen isotherms, J. Am. Chem. Soc., 73 (1951) 373–380.
[29] W.B. Russel, D.A. Saville, W.R. Schowalter, Colloidal Dispersions, Cambridge University Press, 1989.
[30] Y.F. Jia, B. Xiao, K.M. Thomas, Adsorption of metal ions on nitrogen surface functional groups in activated carbons, Langmuir, 18 (2002) 470–478.
[31] F. Hayeeye, M. Sattar, W. Chinpa, O. Sirichote, Kinetics and thermodynamics of Rhodamine B adsorption by gelatin/activated carbon composite beads, Colloids Surf., A, 513 (2017) 259–266.
[32] M. Minamisawa, H. Minamisawa, S. Yoshida, N. Takai, Adsorption behavior of heavy metals on biomaterials, J. Agric. Food Chem., 52 (2004) 5606–5611.
[33] F. Hayeeye, M. Sattar, S. Tekasakul, O. Sirichote, Adsorption of rhodamine B on activated carbon obtained from pericarp of rubber fruit in comparison with the commercial activated carbon, Songklanakarin J. Sci. Technol., 36 (2014) 177–187.
[34] S. Lagergren, Zur theorie der sogenannten adsorption geloster stoffe, K. Sven. Vetensk.akad. Handl., 24 (1898) 1–39.

[35] A. Mellah, S. Chegrouche, M. Barkat, The removal of uranium (VI) from aqueous solutions onto activated carbon: kinetic and thermodynamic investigations, J. Colloid Interface Sci., 296 (2006) 434–441.
[36] Y.S. Ho, G. Mc Kay, Pseudo-second order model for sorption processes, Proc. Biochem., 34 (1999) 451–465.
[37] I. Langmuir, The constitution and fundamental properties of solids and liquids part i. solids, J. Am. Chem. Soc., 38 (1916) 2221–2295.
[38] I. Langmuir, Adsorption of gases on plane surfaces of glass, mica and platinum, J. Am. Chem. Soc., 40 (1918) 1361.
[39] H. Freundlich, Ueber Kolloidfällung und Adsorption, Zeitschrift für Chemie and Industrie der Kolloide, 1 (1907) 321–331.
[40] J. Wang, Y. Kuo, Preparation of fructose-mediated (polyethylene glycol/chitosan) membrane and adsorption of heavy metal ions, J. Appl. Polym. Sci., 105 (2007) 1480–1489.
[41] J. Liu, Y. Ma, Y. Zhang, G. Shao, Novel negatively charged hybrids. 3. Removal of Pb^{2+} from aqueous solution using zwitterionic hybrid polymers as adsorbent, J. Hazard. Mater., 173 (2010) 438–444.
[42] R. Juang, F. Wu, R. Tseng, Characterization and use of activated carbons prepared from bagasses for liquid-phase adsorption, Colloids Surf. A, 201 (2002) 191–199.
[43] J. Li, R. Miller, H. Möhwald, Characterisation of phospholipid layers at liquid interfaces 1. Dynamics of adsorption of phospholipids at the chloroform/water interface, Colloids Surf. A, 114 (1996) 113–121.
[44] J. Wu, J. Li, J. Zhao, R. Miller, Dynamic characterization of phospholipid: protein competitive adsorption at the aqueous solution: chloroform interface, Colloids Surf. A, 175 (2000) 113–120.
[45] Z. Yi, Z. An, G. Cui, J. Li, Stabilized complex film formed by co-adsorption of b-lactoglobulin and phospholipids at liquid/liquid interface, Colloids Surf. A, 223 (2003) 11–16.
[46] Q. He, Y. Zhang, G. Lu, R. Miller, H. Möhwald, J. Li, Dynamic adsorption and characterization of phospholipid and mixed phospholipid/protein layers at liquid/liquid interfaces, Adv. Colloid Interface Sci., 140 (2008) 67–76.
[47] G. Limousin, J.P. Gaudet, L. Charlet, S. Szenknect, V. Barthès, M. Krimissa, Sorption isotherms: a review on physical bases, modeling and measurement, App. Geochem., 22 (2005) 249–275.
[48] S. Rahimi, R.M. Moattari, L. Rajabi, A.A. Derakhshan, Optimization of lead removal from aqueous solution using goethite/chitosan nanocomposite by response surface methodology, Colloids Surf. A, 484 (2015) 216–225.
[49] M. Siahkamari, A. Jamali, A. Sabzevari, A. Shakeria, Removal of lead(II) ions from aqueous solutions using biocompatible polymeric nano-adsorbents: a comparative study, Carbohydr. Polym., 157 (2017) 1180–1189.
[50] X. Peng, F. Xu, W. Zhang, J. Wang, C. Zeng, M. Niu, E. Chmielewská, Magnetic Fe_3O_4@ silica–xanthan gum composites for aqueous removal and recovery of Pb^{2+}, Colloids Surf. A, 443 (2014) 27–36.
[51] L. Jianga, P. Liua, S. Zhaoc, Magnetic ATP/FA/Poly(AA-co-AM) ternary nanocomposite microgel as selective adsorbent for removal of heavy metals from wastewater, Colloids Surf. A, 470 (2015) 31–38.
[52] Y. Wang, L.L. Li, C. Luo, X. Wang, H. Duan, Removal of $Pb^{2+}$from water environment using a novel magnetic chitosan/graphene oxide imprinted Pb^{2+}, Int. J. Biol. Macromol., 86 (2016) 505–511.
[53] A. Jamali, A. Tehrani, F. Shemirani, A. Morsali, Lanthanide metal–organic frameworks as selective microporous materials for adsorption of heavy metal ions, Dalton Trans., 45 (2016) 9193–9200.
[54] Z.Ö.K. Atakl, Y. Yürüm, Synthesis and characterization of anatase nanoadsorbent and application in removal of lead, copper and arsenic from water, Chem. Eng. J., 225 (2013) 625–635.
[55] C. Namasivayam, K. Kadirvelu, Uptake of mercury (II) from wastewater by activated carbon from an unwanted agricultural solid by-product: coirpith, Carbon, 37 (1999) 79–84.
[56] J. Ma, G. Zhou, L. Chu, Y. Liu, C. Liu, S. Luo, Y. Wei, Efficient removal of heavy metal ions with an EDTA functionalized chitosan/polyacrylamide double network hydrogel, ACS Sustain. Chem. Eng., 5 (2017) 843–851.